Synthesis and Characterization of Imidazolate-Bridged Dinuclear Complexes as Active Site Models of Cu,Zn-SOD

Hideki Ohtsu,[1a] Yuichi Shimazaki,[1b] Akira Odani,[1c] Osamu Yamauchi,*[,1b,c] Wasuke Mori,[1d] Shinobu Itoh,[1e] and Shunichi Fukuzumi*[,1a]

Contribution from the Department of Material and Life Science, Graduate School of Engineering, Osaka University, CREST, Japan Science and Technology Corporation (JST), Suita, Osaka 565-0871, Japan, Department of Chemistry, Graduate School of Science, Nagoya University, Chikusa-ku, Nagoya 464-8602, Japan, Research Center for Materials Science, Nagoya University, Chikusa-ku, Nagoya 464-8602, Japan, Department of Chemistry, Faculty of Science, Kanagawa University, 2946 Tsuchiya, Hiratsuka 259-1205, Japan, and Department of Chemistry, Faculty of Science, Osaka City University, Sugimoto, Sumiyoshi-ku, Osaka 558-8585, Japan

Received November 18, 1999

Abstract: New dinucleating ligands having two metal-binding sites bridged by an imidazolate moiety, Hbdpi and HMe_4bdpi (Hbdpi = 4,5-bis(di(2-pyridylmethyl)aminomethyl)imidazole, HMe_4bdpi = 4,5-bis(di(6-methyl-2-pyridylmethyl)aminomethyl)imidazole), have been designed and synthesized as model ligands for copper−zinc superoxide dismutase (Cu,Zn-SOD). The corresponding mononucleating ligand, $MeIm(Py)_2$ ($MeIm(Py)_2$ = ((1-methyl-4-imidazolyl)methyl)bis(2-pyridylmethyl)amine), has also been synthesized for comparison. The imidazolate-bridged Cu(II)−Cu(II) homodinuclear complexes represented as $[Cu_2(bdpi)(CH_3CN)_2](ClO_4)_3\cdot CH_3CN\cdot 3H_2O$ (**1**), $[Cu_2(Me_4bdpi)(H_2O)_2](ClO_4)_3\cdot 4H_2O$ (**2**), a Cu(II)−Zn(II) heterodinuclear complex of the type of $[CuZn(bdpi)(CH_3CN)_2](ClO_4)_3\cdot 2CH_3CN$ (**3**), and a Cu(II) mononuclear complex of $[Cu(MeIm(Py)_2(CH_3CN)](ClO_4)_2\cdot CH_3CN$ (**4**) have been synthesized, and the structures of complexes **1**−**4** were determined by X-ray crystallography. The Cu(II)−Zn(II) distance of 6.197(2) Å in **3** agrees well with that of native Cu,Zn-SOD (6.2 Å). All the metals in **1**−**4** have pentacoordinate geometries with the imidazolate or 1-methylimidazole nitrogen, two pyridine nitrogens, the tertiary amine nitrogen, and a solvent (CH_3CN or H_2O). The coordination site occupied by a solvent can be susceptible to ligand substitution, providing a binding site for substrate superoxide. Magnetic measurements of the Cu(II)−Cu(II) homodinuclear complexes **1** and **2** have shown an antiferromagnetic exchange interaction with a coupling constant of $-2J = 73.4$ and 145.9 cm^{-1}, respectively. The ESR spectra of **1** and **2** exhibited broad signals centered at $g \cong 2.13$ due to the spin−spin interaction between two copper ions, while the ESR spectrum of the Cu(II)−Zn(II) heterodinuclear complex **3** showed a signal which is characteristic of mononuclear trigonal-bipyramidal Cu(II) complexes ($g_{\|} = 2.10$, $g_{\perp} = 2.24$, $|A_{\|}| = 11.7$ mT, and $|A_{\perp}| = 12.4$ mT). The cyclic voltammograms of homodinuclear complexes (**1** and **2**) in CH_3CN gave two reversible waves which correspond to the Cu(I,I)/Cu(I,II) and Cu(I,II)/Cu(II,II) redox processes: $E_{1/2} = -0.31$ and −0.03 V vs Ag/AgCl for **1** and $E_{1/2} = -0.29$ and +0.12 V vs Ag/AgCl for **2**, respectively. On the other hand, the Cu(II)−Zn(II) heterodinuclear complex **3** exhibited one Cu(I)/(II) reversible wave, $E_{1/2} = -0.03$ V vs Ag/AgCl, which is shifted in a positive direction (0.21 and 0.19 V) as compared to those of the corresponding Cu(II) mononuclear complexes. All the examined complexes catalyzed the dismutation of superoxide at biological pH; the SOD activity increased in the order **2** < **1** < **3**.

Introduction

The biological activity of metalloproteins is usually associated with a particular coordination environment of the metal active site.[2] For example, copper−zinc superoxide dismutase (Cu,Zn-SOD) contains an imidazolate-bridged Cu(II)−Zn(II) heterodinuclear metal center in its active site.[3−8] This enzyme catalyzes a very rapid two-step dismutation of superoxide to dioxygen and hydrogen peroxide through an alternate reduction and oxidation of the active-site copper ion.[7,8] The biological function of SOD is known to play a very important role in preventing oxidative damage by the anticancer and antiaging mechanisms.[9−11] The copper ion is coordinated to four imidazole N atoms of

(1) (a) Osaka University. (b) Department of Chemistry, Nagoya University. (c) Research Center for Materials Science, Nagoya University. (d) Kanagawa University. (e) Osaka City University.

(2) (a) Lippard, S. J. *Science* **1993**, *261*, 699. (b) Kaim, W.; Schwederski, B. *Bioinorganic Chemistry: Inorganic Elements in the Chemistry of Life*; John Wiley & Sons: New York, 1991.

(3) (a) Fridovich, I. *J. Biol. Chem.* **1989**, *264*, 7761. (b) Fridovich, I. *Annu. Rev. Biochem.* **1995**, *64*, 97.

(4) Bertini, I.; Banci, L.; Piccioli, M. *Coord. Chem. Rev.* **1990**, *100*, 67.

(5) Tainer, J. A.; Getzoff, E. D.; Beem, K. M.; Richardson, J. S.; Richardson, D. C. *J. Mol. Biol.* **1982**, *160*, 181.

(6) Tainer, J. A.; Getzoff, E. D.; Richardson, J. S.; Richardson, D. C. *Nature* **1983**, *306*, 284.

(7) Fielden, E. M.; Roberts, P. B.; Bray, R. C.; Lowe, D. J.; Mautner, G. N.; Rotilio, G.; Calabrese, L. *Biochem. J.* **1974**, *139*, 49.

(8) (a) Ellerby, L. M.; Cabelli, D. E.; Graden, J. A.; Valentine, J. S. *J. Am. Chem. Soc.* **1996**, *118*, 6556. (b) Hart, P. J.; Balbirnie, M. M.; Ogihara, N. L.; Nersissian, A. M.; Weiss, M. S.; Valentine, J. S.; Eisenberg, D. A. *Biochemistry* **1999**, *38*, 2167.

(9) Oberley, L. W.; Buettner, G. R. *Cancer Res.* **1979**, *39*, 1141.

(10) Farmer, K. J.; Sohal, R. S. *Free Radical Biol. Med.* **1989**, *7*, 23.

(11) Rusting, R. L. *Sci. Am.* **1992**, *267*, 88.

10.1021/ja994050j CCC: $19.00 © 2000 American Chemical Society
Published on Web 06/06/2000

histidine residues in a distorted square-pyramidal geometry, while the zinc ion located at a distance of 6.2 Å from the copper ion is coordinated to a carboxylato O atom of an aspartic acid residue and three imidazole N atoms of histidine residues in a distorted tetrahedral structure.[3,4] The copper ion is absolutely essential for the SOD activity,[12] while the roles of imidazolate bridge and zinc ion remain less understood.

A number of imidazolate-bridged Cu(II)−Cu(II) homodinuclear complexes have been designed and synthesized as SOD mimics,[13−27] since the pioneering work of Lippard et al.[13] provided valuable insights into the structure and function of the Cu,Cu-SOD active site. In contrast to these studies on the Cu(II)−Cu(II) homodinuclear complexes, only a few imidazolate-bridged heterodinuclear Cu,Zn-SOD model complexes have been reported.[27] The heterodinuclear Cu,Zn-SOD model complexes have so far been constructed by the self-assembly strategy using two independent mononuclear complexes and a bridging imidazolate ring.[27] The inherent instability of such complexes has precluded detailed examinations of the SOD functions. Since Cu(II)−Zn(II) heterodinuclear complexes reported so far have pentacoordinate metal sites with four N atoms from the ligand and one N atom from the bridging imidazolate, there is no binding site for superoxide, which is essential in the active site of the native enzyme.

We report herein the synthesis, the X-ray crystal structure determination, the results of magnetic susceptibility, ESR and electronic spectroscopic investigations, and the electrochemistry of imidazolate-bridged Cu(II)−Cu(II) homodinuclear and Cu(II)−Zn(II) heterodinuclear complexes containing new dinucleating ligands, Hbdpi and HMe_4bdpi (Hbdpi = 4,5-bis(di(2-pyridylmethyl)aminomethyl)imidazole,[28] HMe_4bdpi = 4,5-bis(di(6-methyl-2-pyridylmethyl)aminomethyl)imidazole). The corresponding mononuclear Cu(II) complex with mononucleating ligand, $MeIm(Py)_2$ ($MeIm(Py)_2$ = ((1-methyl-4-imidazolyl)methyl)bis(2-pyridylmethyl)amine), has also been synthesized and the spectroscopic properties are compared with those of the dinuclear complexes. The coordination site available for the binding of superoxide is clearly shown by the X-ray structures of the Cu(II)−Cu(II) homodinuclear and Cu(II)−Zn(II) heterodinuclear complexes, both of which have the same coordination geometry. A comparison between the Cu(II)−Cu(II) homodinuclear and Cu(II)−Zn(II) heterodinuclear complexes has allowed us to clarify the roles of zinc ion and imidazolate bridge in Cu,Zn-SOD. The SOD activity of these complexes was also examined to show the highest activity among the reported SOD models, the structures of which are well characterized.[17,26,27d]

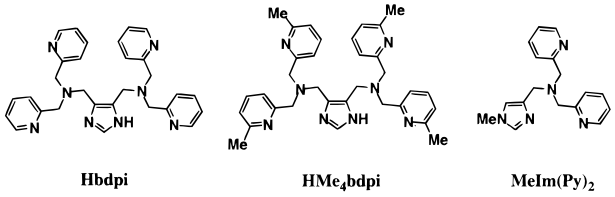

Experimental Section

Materials. All chemicals used for the ligand synthesis were commercial products of the highest available purity and were further purified by the standard methods.[29] Solvents were also purified by standard methods before use.[29]

Synthesis of Ligands. All ligands used in this study were prepared according to the following procedures, and the structures of the products were confirmed by the analytical data (vide infra).

4,5-Bis(di(2-pyridylmethyl)aminomethyl)imidazole (Hbdpi). Bis(2-pyridylmethyl)amine (3.2 g, 16 mmol) and a small amount of acetic acid were added to a methanol solution (100 mL) containing imidazole-4,5-dialdehyde (1.0 g, 8 mmol). To the methanol solution was added dropwise sodium cyanoborohydride (1.0 g, 16 mmol). After the resulting solution had been stirred for 3 days at room temperature, it was acidified with concentrated hydrochloric acid and concentrated to dryness under reduced pressure. The residue was dissolved in a saturated aqueous solution of Na_2CO_3 (50 mL) and extracted with three 50 mL portions of chloroform. The combined extracts were dried over Na_2SO_4 and after removal of the solvent gave a brown oily product, which was purified by silica gel chromatography with chloroform/methanol as eluent to give Hbdpi. Yield: 3.16 g (80.0%). ^{1}H NMR ($CDCl_3$, 400 MHz): δ = 3.65 (s, 4H, NCH_2Im, Im = imidazole moiety), 3.75 (s, 8H, NCH_2Py, Py = pyridine moiety), 7.12 (m, 4H, Py), 7.47 (d, 4H, Py, J = 6.8 Hz), 7.61 (td, 4H, Py, J = 2.0, 8.0 Hz), 7.66 (s, 1H, Im), 8.51 (d, 4H, Py, J = 5.2 Hz). ^{13}C NMR ($CDCl_3$, 100 MHz): δ = 48.2 (CH_2), 59.2 (CH_2), 121.7 (Py), 122.0 (Im), 123.2 (Py), 133.8 (Im), 136.2 (Py), 148.4 (Py), 158.9 (Py).

4,5-Bis(di(6-methyl-2-pyridylmethyl)aminomethyl)imidazole (HMe_4bdpi). The same procedure as that for the synthesis of Hbdpi was applied to obtain HMe_4bdpi using bis(6-methyl-2-pyridylmethyl)amine (3.66 g, 16 mmol) instead of bis(2-pyridylmethyl)amine. Yield: 2.82 g (64.1%). ^{1}H NMR ($CDCl_3$, 400 MHz): δ = 2.51 (s, 12H, CH_3), 3.64 (s, 4H, NCH_2Im), 3.71 (s, 8H, NCH_2Py), 6.96 (d, 4H, Py, J = 8.0 Hz), 7.30 (d, 4H, Py, J = 8.8 Hz), 7.49 (t, 4H, Py, J = 7.6 Hz), 7.64 (s, 1H, Im). ^{13}C NMR ($CDCl_3$, 100 MHz): δ = 23.9 (CH_3), 48.2 (CH_2), 59.4 (CH_2), 120.0 (Py), 121.1 (Im), 121.2 (Py), 133.7 (Im), 136.4 (Py), 157.1 (Py), 158.3 (Py).

((1-Methyl-4-imidazolyl)methyl)bis(2-pyridylmethyl)amine ($MeIm(Py)_2$). Bis(2-pyridylmethyl)amine (1.6 g, 8 mmol) and a small amount of acetic acid were added to a methanol solution (100 mL)

(12) McCord, J. M.; Fridovich, I. *J. Biol. Chem.* **1969**, *244*, 6049.
(13) (a) Kolks, G.; Frihart, C. R.; Rabinowitz, H. N.; Lippard, S. J. *J. Am. Chem. Soc.* **1976**, *98*, 5720. (b) O'Young, C.-L.; Dewan, J. C.; Lilienthal, H. R.; Lippard, S. J. *J. Am. Chem. Soc.* **1978**, *100*, 7291. (c) Coughlin, P. K.; Dewan, J. C.; Lippard, S. J.; Watanabe, E.; Lehn, J.-M. *J. Am. Chem. Soc.* **1979**, *101*, 265. (d) Davis, W. M.; Dewan, J. C.; Lippard, S. J. *Inorg. Chem.* **1981**, *20*, 2933. (e) Kolks, G.; Lippard, S. J.; Waszczak, J. V.; Lilienthal, H. R. *J. Am. Chem. Soc.* **1982**, *104*, 717. (f) Coughlin, P. K.; Martin, A. E.; Dewan, J. C.; Watanabe, E.; Bulkowski, J. E.; Lehn, J. L.; Lippard, S. J. *Inorg. Chem.* **1984**, *23*, 1004. (g) Coughlin, P. K.; Lippard, S. J. *Inorg. Chem.* **1984**, *23*, 1446.
(14) Strotkamp, K. G.; Lippard, S. J. *Acc. Chem. Res.* **1982**, *15*, 318.
(15) Murphy, B. P. *Coord. Chem. Rev.* **1993**, *124*, 63.
(16) Gartner, A.; Weser, U. *Top. Curr. Chem.* **1986**, *132*, 1.
(17) Weser, U.; Schubotz, L. M.; Lengfelder, E. *J. Mol. Catal.* **1981**, *13*, 249.
(18) Hendricks, H. M. J.; Birker, P. J. W. L.; Verschoor, G. C.; Reedjik, J. *J. Chem. Soc., Dalton Trans.* **1982**, 623.
(19) Costes, J. P.; Serra, J. F.; Dahan, F.; Laurent, J. P. *Inorg. Chem.* **1986**, *25*, 2790.
(20) Drew, M. G. B.; Cairns, C.; Lavery, A.; Nelson, S. M. *J. Chem. Soc., Chem. Commun.* **1980**, 1122.
(21) Drew, M. G. B.; McCann, S. M.; Nelson, S. M. *J. Chem. Soc., Dalton Trans.* **1981**, 1868.
(22) Drew, M. G. B.; Nelson, S. M.; Reedijk, J. *Inorg. Chim. Acta* **1982**, *64*, L189.
(23) Salata, C. A.; Youinou, M. T.; Burrows, C. J. *J. Am. Chem. Soc.* **1989**, *111*, 9278.
(24) Salata, C. A.; Youinou, M. T.; Burrows, C. J. *Inorg, Chem.* **1991**, *30*, 3454.
(25) Kimura, E.; Kurogi, Y.; Shionoya, M.; Shiro, M. *Inorg. Chem.* **1991**, *30*, 4524.
(26) Tabbi, G.; Driessen, W. L.; Reedijk, J.; Bonomo, R. P.; Veldman, N.; Spek, A. L. *Inorg. Chem.* **1997**, *36*, 1168.
(27) (a) Sato, M.; Nagae, S.; Uehara, M.; Nakaya, J. *J. Chem. Soc., Chem. Commun.* **1984**, 1661. (b) Lu, Q.; Luo, Q. H.; Dai, A. B.; Zhou, Z. Y.; Hu, G. Z. *J. Chem. Soc., Chem. Commun.* **1990**, 1429. (c) Zongwan, M.; Dong, C.; Wenxia, T.; Kaibei, Y.; Li, L. *Polyhedron* **1992**, *11*, 191. (d) Pierre, J.-L.; Chautemps, P.; Refaif, S.; Beguin, C.; Marzouki, A. E.; Serratrice, G.; Saint-Aman, E.; Rey, P. *J. Am. Chem. Soc.* **1995**, *117*, 1965. (e) Mao, Z.-W.; Chen, M.-Q.; Tan, X.-S.; Liu, J.; Tang, W.-X. *Inorg. Chem.* **1995**, *34*, 2889.
(28) For a preliminary report, see: Ohtsu, H.; Shimazaki, Y.; Odani, A.; Yamauchi, O. *J. Chem. Soc., Chem. Commun.* **1999**, 2393.
(29) Perrin, D. D.; Armarego, W. L. F.; Perrin, D. R. *Purification of Laboratory Chemicals*; Pergamon Press: Elmsford, 1966.

Table 1. Crystal Data for Complexes **1**, **2**, **3**, and **4**

	1	**2**	**3**	**4**
formula	$Cu_2O_{15}C_{35}H_{44}Cl_3N_{11}$	$Cu_2O_{18}C_{33}H_{49}Cl_3N_8$	$CuZnO_{12}C_{37}H_{41}Cl_3N_{12}$	$CuO_8C_{21}H_{25}Cl_2N_7$
formula weight	1092.25	1079.24	1081.09	637.92
color	green	green	green	green
crystal size/mm	0.15 × 0.21 × 0.27	0.04 × 0.05 × 0.15	0.09 × 0.09 × 0.15	0.30 × 0.30 × 0.40
crystal system	triclinic	monoclinic	triclinic	monoclinic
space group	$P\bar{1}$	$P2_1/n$	$P\bar{1}$	$P2_1/n$
a/Å	14.475(2)	9.843(2)	14.447(1)	14.861(5)
b/Å	14.554(2)	18.361(2)	14.561(1)	10.784(5)
c/Å	12.270(1)	25.111(3)	12.214(1)	35.597(4)
α/deg	108.474(8)		108.002(7)	
β/deg	107.348(8)	97.84(2)	106.920(7)	90.57(2)
γ/deg	89.14(1)		89.069(7)	
V/Å^3	2331.2(5)	4495(1)	2330.3(4)	5704(3)
Z	2	4	2	8
D_c/g cm^{-3}	1.684	1.676	1.508	1.485
radiation	Cu Kα (λ = 1.54178 Å)	Cu Kα (λ = 1.54178 Å)	Cu Kα (λ = 1.54178 Å)	Mo Kα (λ = 0.71069 Å)
μ/cm^{-1}	34.64	34.42	34.30	10.08
F(000)/e	1208.00	2004.00	1138.00	2616.00
scan method	$\omega - 2\theta$	$\omega - 2\theta$	$\omega - 2\theta$	$\omega - 2\theta$
$2\theta_{max}$/deg	120.02	136.2	110.2	50.2
scan speed/deg min^{-1}	16.0	4.0	8.0	16.0
scan range/deg	1.73 + 0.30 tan θ	1.73 + 0.30 tan θ	1.31 + 0.30 tan θ	0.79 + 0.30 tan θ
observed reflections	6033	8603	5067	7925
independent reflections	5761 (R_{int} = 0.037)	8059 (R_{int} = 0.038)	4821 (R_{int} = 0.034)	7786 (R_{int} = 0.026)
reflections used	5761	7792	4821	7786
no. of variables	596	578	596	704
R^a ($I > 2.00\sigma(I)$)	0.073	0.084	0.074	0.075
$R_w{}^a$ ($I > 2.00\sigma(I)$)	0.109	0.132	0.110	0.105

[a] $R = \sum||F_o| - |F_c||/\sum|F_o|$; $R_w = [\sum w(|F_o| - |F_c|)^2/\sum w|F_o|^2]^{1/2}$; $w = 1/\sigma^2(|F_o|)$.

containing 1-methyl imidazole-4-aldehyde (0.88 g, 8 mmol). To the methanol solution was added dropwise sodium cyanoborohydride (0.5 g, 8 mmol). After the resulting solution had been stirred for 3 days at room temperature, it was acidified with concentrated hydrochloric acid and concentrated to dryness under a reduced pressure. The residue was dissolved in a saturated aqueous solution of Na_2CO_3 (50 mL) and extracted with three 50 mL portions of chloroform. The combined extracts were dried over Na_2SO_4 and after removal of the solvent gave a brown oily product, which was purified by silica gel chromatography with chloroform/methanol as eluent to give Hbdpi. Yield: 2.0 g (85.3%). ^{1}H NMR ($CDCl_3$, 400 MHz): δ = 3.61 (s, 3H, CH_3), 3.70 (s, 2H, NC*H*$_2$Im), 3.86 (s, 4H, NC*H*$_2$Py), 6.87 (s, 1H, Im), 7.11 (m, 2H, Py), 7.37 (s, 1H, Im), 7.64 (m, 4H, Py), 7.66 (s, 1H, Im), 8.50 (m, 2H, Py). ^{13}C NMR ($CDCl_3$, 100 MHz): δ = 32.8 (CH_3), 51.1 (CH_2), 59.2 (CH_2), 118.6 (Im), 121.4 (Py), 122.6 (Py), 136.0 (Py), 136.9 (Im), 138.6 (Im), 148.4 (Py), 159.4 (Py).

[Cu$_2$(bdpi)(CH$_3$CN)$_2$](ClO$_4$)$_3$·CH$_3$CN·3H$_2$O (1). To a methanol solution (10 mL) of Hbdpi (0.49 g, 1.0 mmol) was added dropwise 2 equiv of $Cu(ClO_4)_2$·$6H_2O$ (0.74 g, 2.0 mmol) in methanol (10 mL), and a few drops of triethylamine was then added to the resulting solution. After the solution was left to stand for a few days at room temperature, microcrystals precipitated; these were isolated and recrystallized from CH_3CN. Yield: 0.692 g (67%). Anal. Calcd for $C_{31}H_{32}N_9Cu_2Cl_3O_{12}$: C, 38.94; H, 3.37; N, 13.18; Cu, 13.29. Found: C, 38.95; H, 3.32; N, 13.35; Cu, 13.27. MS data: m/z 815 [M − ClO_4]$^+$.

[Cu$_2$(Me$_4$bdpi)(H$_2$O)$_2$](ClO$_4$)$_3$·4H$_2$O (2) was prepared in the same manner as **1** using the HMe$_4$bdpi ligand instead of Hbdpi. Yield: 0.745 g (74%). Anal. Calcd for $C_{33}H_{41}N_8Cu_2Cl_3O_{14}$: C, 39.35; H, 4.10; N, 11.13; Cu, 12.62. Found: C, 39.42; H, 4.08; N, 11.37; Cu, 12.58. MS data: m/z 871 [M − ClO_4]$^+$.

[CuZn(bdpi)(CH$_3$CN)$_2$](ClO$_4$)$_3$·2CH$_3$CN (3). To a methanol solution (10 mL) of Hbdpi (0.49 g, 1.0 mmol) was added dropwise $Cu(ClO_4)_2$·$6H_2O$ (0.37 g, 1.0 mmol) and $Zn(ClO_4)_2$·$6H_2O$(0.37 g, 1.0 mmol) in methanol (10 mL). To the resulting solution was added a few drops of triethylamine. After being left to stand for a few days at room temperature, the solution precipitated microcrystals, which were isolated and recrystallized from CH_3CN. Yield: 0.724 g (67%). Anal. Calcd for $C_{29}H_{35}N_8Cu_1Zn_1Cl_3O_{15}$: C, 35.87; H, 3.63; N, 11.54; Cu, 6.54; Zn, 6.73. Found: C, 35.88; H, 3.56; N, 11.77; Cu, 6.46; Zn, 6.66. The ratio of Cu to Zn in complex **3** was determined with ICP (SEIKODENKO SPS-700) using the standard solutions (1000 ppm) of Cu(II) and Zn(II) obtained from Nacalai Tesque. MS data: m/z 816 [M − ClO_4]$^+$.

[Cu(MeIm(Py)$_2$)(CH$_3$CN)](ClO$_4$)$_2$·CH$_3$CN (4). To a methanol solution (10 mL) of MeIm(Py)$_2$ (0.29 g, 1.0 mmol) was added dropwise $Cu(ClO_4)_2$·$6H_2O$ (0.37 g, 1.0 mmol) in methanol (10 mL). After the solution was left to stand for a few days at room temperature, microcrystals precipitated; these were isolated and recrystallized from CH_3CN. Yield: 0.370 g (60%). Anal. Calcd for $C_{31}H_{32}N_9Cu_2Cl_3O_{12}$: C, 38.23; H, 3.72; N, 14.08. Found: C, 38.57; H, 3.77; N, 14.79. MS data: m/z 455 [M − ClO_4]$^+$.

X-ray Structure Determination. The syntheses of complexes **1**, **2**, **3**, and **4** afforded well-shaped crystals suitable for X-ray diffraction study. The X-ray experiments were carried out on a Rigaku AFC-5R four-circle automated diffractometer with graphite-monochromated Cu Kα radiation and rotating anode generator except for complex **4**, for which Mo Kα radiation was used. The crystals were mounted on the glass capillary. The reflection intensities for **1**, **2**, **3**, and **4** were monitored by three standard reflections every 2 h and 150 measurements. The intensity decay for all the crystals was within 2%. Reflection data were corrected for both Lorentz and polarization effects. DIFABS correction was applied except for complex **4**, because the absorption coefficients (μ) for all crystals were slightly large. The structure was solved using the heavy-atom method and refined anisotropically for non-hydrogen atoms by full-matrix least-squares calculations. Each refinement was continued until all shifts were smaller than one-third of the standard deviations of the parameters involved. Atomic scattering factors were taken from the literature.[30] All hydrogen atoms were located at the calculated positions except for those of water molecules, and they were assigned a fixed displacement and constrained to ideal geometry with C−H = 0.95 Å. The thermal parameters of calculated hydrogen atoms were related to those of their parent atoms by U(H) = 1.2U_{eq}(C,N). The hydrogen atoms of water molecules were located from the difference Fourier maps. All the calculations were performed by using the TEXSAN crystallographic software program package from Molecular Structure Corp. Summaries of the fundamental crystal data and experimental parameters for the structure determination of complexes **1**, **2**, **3**, and **4** are given in Table 1.

(30) *International Tables for X-ray Crystallography*; Kynoch Press: Birmingham, U.K., 1974; Vol. IV.

Magnetic Measurements. Variable-temperature magnetic susceptibility data were measured on a polycrystalline sample of complexes **1** and **2** using a model HOXSAN HSM-D SQUID susceptometer in the temperature range 5−300 K with an applied field of 10.0 kG. The polycrystalline sample was embedded in Parafilm to prevent torquing of the crystallites in an external field. A diamagnetic correction, estimated from Pascal's constants, was subtracted from the experimental susceptibilities to give the molar paramagnetic susceptibilities.

Spectroscopies. Electronic spectra were measured with a Shimadzu UV-3101PC spectrophotometer. NMR measurements were performed with a JEOL JNM-GSX-400 (400 MHz) NMR spectrometer. Frozen solution ESR spectra were taken on a JEOL JES-RE1X X-band spectrometer, equipped with a standard low-temperature apparatus. All the spectra were recorded at 77 K in quartz tubes with a 4-mm inner diameters. The *g* values were calibrated with a Mn(II) marker used as a reference.

Electrochemistry. Redox potentials of complexes **1**, **2**, **3**, and **4** (1.0 mM) in dried CH_3CN containing 0.1 M tetra-*n*-butylammonium perchlorate (TBAP) as supporting electrolyte were determined at room temperature by cyclic voltammetry using a three-electrode system under deaerated conditions and a BAS 100B electrochemical analyzer. A glassy-carbon and platinum wire were used as the working electrode and the counter electrode, respectively. The reversibility of the electrochemical processes was evaluated by standard procedures, and all potentials were recorded against a Ag/AgCl reference electrode which was calibrated using the ferrocene/ferrocenium redox couple.

SOD Activities. Superoxide anion was generated in situ by the xanthine−xanthine oxidase system and detected spectrophotometrically by reduction of ferricytochrome *c*. The assay was carried out in γ-collidine buffer (50 mM, pH 7.77, 25.0 °C) containing 10 μM ferricytochrome *c*, 50 μM xanthine, and an appropriate amount of xanthine oxidase to cause a change in absorbance at 550 nm ($\Delta A_{550} = 0.025$ min^{-1}). The IC_{50} values are defined as the 50% inhibition concentration of cytochrome *c* reduction. Before the assay, we examined whether Cu(II) and its complexes used in the present investigation inhibited xanthine oxidase by use of the maximum at 295 nm due to uric acid at pH 7.77 as reported,[31] and we concluded that they did not inhibit xanthine oxidase under the experimental conditions.

Results and Discussion

Preparation and Characterization of Imidazolate-Bridged Cu(II)−Cu(II) Homodinuclear Complexes, Cu(II)−Zn(II) Heterodinuclear Complexes, and the Cu(II) Mononuclear Complex. $Cu(ClO_4)_2$ and the Hbdpi ligand were mixed in a 2:1 ratio in methanol, and then to the resulting solution was added triethylamine. This procedure enabled us to isolate the Cu(II)−Cu(II) homodinuclear complex **1** (see Experimental Section). In the same manner complex **2** was obtained using the HMe_4bdpi ligand instead of Hbdpi. In this case complex **2** was also obtained without triethylamine.

When equimolar amounts of $Cu(ClO_4)_2$ and $Zn(ClO_4)_2$ are employed in the reaction with 1 equiv of Hbdpi in the presence of triethylamine, heterodinuclear complex **3** is crystallized selectively from CH_3CN. Without triethylamine, however, neither complex **1** nor **3** could be isolated. Complex **3** was identified by elemental analysis and FAB^+ mass spectrometry (see Experimental Section). The observation of $m/z = 816$ in the mass spectrum clearly demonstrates formation of the heterodinuclear complex **3** rather than a mixture of homodinuclear copper and zinc complexes. The Cu(II):Zn(II) ratio in complex **3** was also confirmed by the ICP measurements (see Experimental Section). This is the first example of formation of an imidazolate-bridged Cu(II)−Zn(II) heterodinuclear complex via the direct reaction between the ligand and metal ions. When the Hbdpi ligand was replaced by HMe_4bdpi, however, Cu(II)−Zn(II) heterodinuclear complex could not be isolated due to nonselective formation of the Cu(II)−Cu(II) and Zn(II)−Zn(II) homodinuclear complexes.

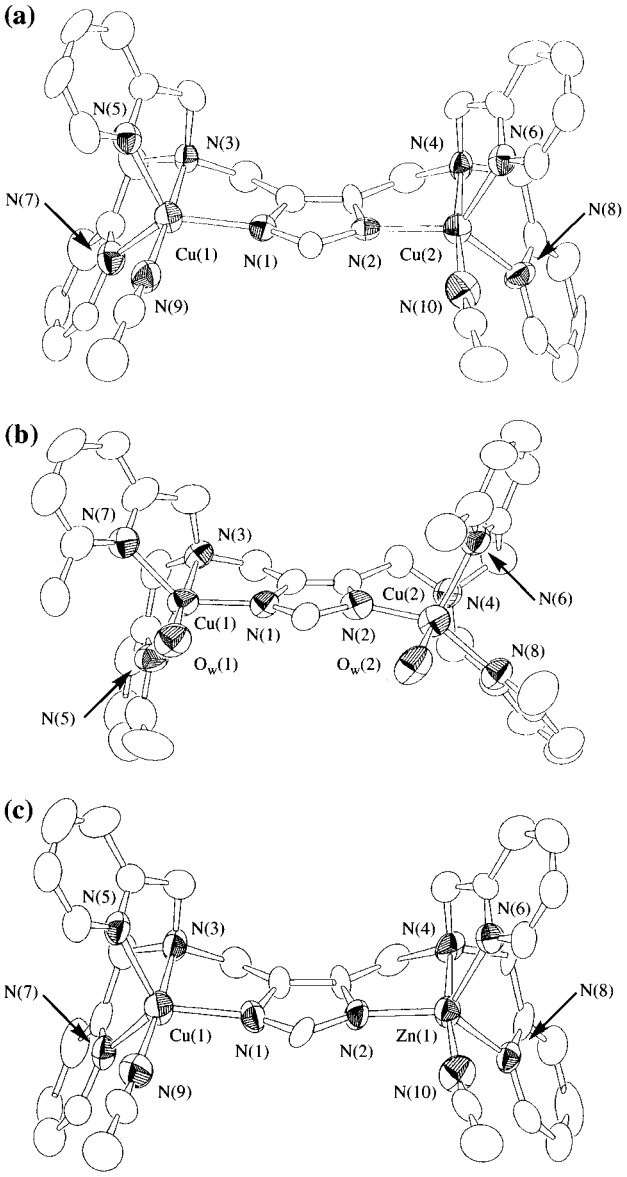

Figure 1. ORTEP views of dinuclear complexes of (a) $[Cu_2(bdpi)(CH_3CN)_2](ClO_4)_3\cdot CH_3CN\cdot 3H_2O$ (**1**), (b) $[Cu_2(Me_4bdpi)(H_2O)_2](ClO_4)_3\cdot 4H_2O$ (**2**), and (c) $[CuZn(bdpi)(CH_3CN)_2](ClO_4)_3\cdot 2CH_3CN$ (**3**). The hydrogen atoms are omitted for clarity.

A mononuclear Cu(II) complex with a mononucleating ligand, $[Cu(MeIm(Py)_2)(CH_3CN)](ClO_4)_2\cdot CH_3CN$ (**4**), was obtained by the reaction of $Cu(ClO_4)_2$ with $MeIm(Py)_2$ in methanol (see Experimental Section).

Crystal Structures. ORTEP views of the dinuclear complexes **1**, **2**, and **3** are shown in Figure 1 (parts a, b, and c, respectively), and the mononuclear complex **4**[32] is shown in Figure 2. Selected bond distances and angles of complexes **1**, **2**, **3**, and **4** are summarized in Tables 2, 3, 4, and 5, respectively.

The two copper ions in Cu(II)−Cu(II) homodinuclear complexes **1** and **2** have a pentacoordinate structure including a solvent molecule which can be readily replaced by a substrate as shown in Figure 1 (parts a and b, respectively). Complexes

(31) (a) Chang, W. S.; Lee, Y. J.; Lu, F. J.; Chiang, H. C. *Anticancer Res.* **1993**, *13*, 2165. (b) Cotell, N.; Bernier, J. L.; Henichart, J. P.; Catteau, J. P.; Gaydou, E.; Wallet, J. C. *Free Rad. Biol. Med.* **1992**, *13*, 221.

(32) The X-ray analysis shows that there are two independent molecules (molecules 1 and 2) of complex **4** in an ansymmetric unit, as shown in Table 5. Their main structural features and metric parameters are nearly identical.

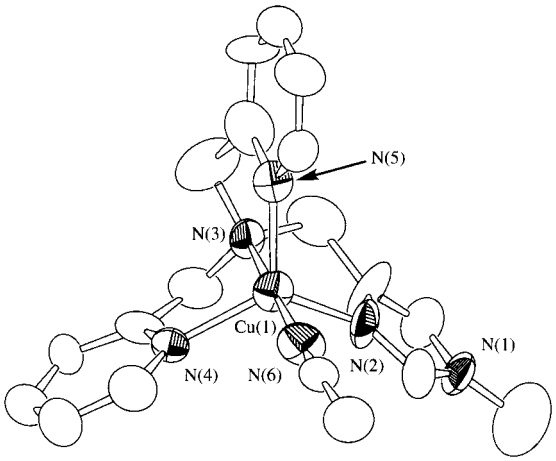

Figure 2. ORTEP view of a mononuclear complex of [Cu(MeIm-$(Py)_2$)(CH_3CN)]$(ClO_4)_2$·CH_3CN (**4**). One of the two crystallographically independent molecules of **4** is drawn (molecule 1).[32] The hydrogen atoms are omitted for clarity.

Table 2. Selected Bond Distances and Angles of Complex **1**

Bond Distances (Å)			
Cu(1)−N(1)	2.006(8)	Cu(2)−N(2)	2.008(8)
Cu(1)−N(3)	2.037(8)	Cu(2)−N(4)	2.026(8)
Cu(1)−N(5)	2.085(10)	Cu(2)−N(6)	2.111(9)
Cu(1)−N(7)	2.096(9)	Cu(2)−N(8)	2.060(9)
Cu(1)−N(9)	1.993(9)	Cu(2)−N(10)	1.977(9)
Bond Angles (deg)			
N(1)−Cu(1)−N(3)	82.7(3)	N(2)−Cu(2)−N(4)	83.1(3)
N(1)−Cu(1)−N(5)	121.0(3)	N(2)−Cu(2)−N(6)	119.8(3)
N(1)−Cu(1)−N(7)	121.7(3)	N(2)−Cu(2)−N(8)	123.1(3)
N(1)−Cu(1)−N(9)	100.6(4)	N(2)−Cu(2)−N(10)	101.9(3)
N(3)−Cu(1)−N(5)	82.1(4)	N(4)−Cu(2)−N(6)	81.6(3)
N(3)−Cu(1)−N(7)	81.6(3)	N(4)−Cu(2)−N(8)	81.7(3)
N(3)−Cu(1)−N(9)	176.4(3)	N(4)−Cu(2)−N(10)	175.0(3)
N(5)−Cu(1)−N(7)	111.7(3)	N(6)−Cu(2)−N(8)	111.6(3)
N(5)−Cu(1)−N(9)	97.3(4)	N(6)−Cu(2)−N(10)	95.9(4)
N(7)−Cu(1)−N(9)	95.3(4)	N(8)−Cu(2)−N(10)	95.3(4)

Table 3. Selected Bond Distances and Angles of Complex **2**

Bond Distances (Å)			
Cu(1)−N(1)	1.968(7)	Cu(2)−N(2)	1.973(8)
Cu(1)−N(3)	2.027(7)	Cu(2)−N(4)	2.039(8)
Cu(1)−N(5)	2.198(10)	Cu(2)−N(6)	2.186(10)
Cu(1)−N(7)	2.089(8)	Cu(2)−N(8)	2.080(7)
Cu(1)−O_w(1)	1.995(6)	Cu(2)−O_w(2)	1.973(7)
Bond Angles (deg)			
N(1)−Cu(1)−N(3)	84.0(3)	N(2)−Cu(2)−N(4)	83.2(3)
N(1)−Cu(1)−N(5)	110.1(3)	N(2)−Cu(2)−N(6)	109.4(4)
N(1)−Cu(1)−N(7)	140.2(3)	N(2)−Cu(2)−N(8)	138.8(4)
N(1)−Cu(1)−O_w(1)	95.0(3)	N(2)−Cu(2)−O_w(2)	93.8(3)
N(3)−Cu(1)−N(5)	80.0(4)	N(4)−Cu(2)−N(6)	80.5(3)
N(3)−Cu(1)−N(7)	80.1(3)	N(4)−Cu(2)−N(8)	79.8(3)
N(3)−Cu(1)−O_w(1)	171.7(4)	N(4)−Cu(2)−O_w(2)	169.2(4)
N(5)−Cu(1)−N(7)	102.8(3)	N(6)−Cu(2)−N(8)	104.8(3)
N(5)−Cu(1)−O_w(1)	108.0(3)	N(6)−Cu(2)−O_w(2)	110.3(4)
N(7)−Cu(1)−O_w(1)	95.6(3)	N(8)−Cu(2)−O_w(2)	96.0(3)

1 and **2** have a bridged imidazolate between the two Cu(II) ions with a Cu(1)−N(1) distance of 2.006(8) and 1.968(7) Å, and a Cu(2)−N(2) distance of 2.008(8) and 1.973(8) Å, respectively. Each of the Cu sites coordinates the imidazolate nitrogen, two pyridine nitrogens, the tertiary amine nitrogen, and a solvent nitrogen (acetonitrile) or oxygen (water).

Complex **1** has C_{2v} symmetry through C(2) to the center of C(4)−C(5) in a bridged imidazolate, while **2** has only C_2 symmetry. Thus, complex **1** has higher symmetry than **2**. The basal plane at the Cu center comprises two pyridine nitrogens and a bridged imidazolate nitrogen. The relative amounts of the trigonal-bipyramidal component are indicated by an indexing τ representing the degree of trigonality within the structural continuum between square-pyramidal ($\tau = 0$) and trigonal-bipyramidal structures ($\tau = 1$).[33] The τ values for two Cu(II) ions of complex **1** are obtained as $\tau_1 = 0.92$ and $\tau_2 = 0.87$ by using the equation $\tau = (\beta - \alpha)/60$, where α_1 = N(1)−Cu(1)−N(5) (121.0°), β_1 = N(3)−Cu(1)−N(9) (176.4°), α_2 = N(2)−Cu(2)−N(8) (123.1°), and β_2 = N(4)−Cu(2)−N(10) (175.0°), respectively. Thus, the coordination environment of each Cu(II) of complex **1** is a slightly distorted trigonal-bipyramidal structure in which the threefold axis is comprised of N(1), N(5), and N(7) atoms (or N(2), N(6), and N(8) atoms), with the axial atoms N(3) and N(9) (or N(4) and N(10)).

The structure of complex **2** is different from that of **1** with respect to the coordination environment of the Cu(II) center. The τ values for two Cu(II) ions of complex **2** are obtained as $\tau_1 = 0.53$ and $\tau_2 = 0.51$ by using the equation $\tau = (\beta - \alpha)/60$, where α_1 = N(1)−Cu(1)−N(7) (140.2°), β_1 = N(3)−Cu(1)−O_w(1) (171.7°), α_2 = N(2)−Cu(2)−N(8) (138.8°), β_2 = N(4)−Cu(2)−O_w(2) (169.2°), respectively. Thus, the geometry of copper ions in complex **2** can be described as a distorted square-pyramidal structure in which the C_4 axis is comprised of N(1), N(3), N(7), and O_w(1) atoms (or N(2), N(4), N(8), and

Table 4. Selected Bond Distances and Angles of Complex **3**

Bond Distance (Å)			
Cu(1)−N(1)	1.998(7)	Zn(1)−N(2)	2.002(7)
Cu(1)−N(3)	2.101(7)	Zn(1)−N(4)	2.112(7)
Cu(1)−N(5)	2.068(7)	Zn(1)−N(6)	2.091(9)
Cu(1)−N(7)	2.092(8)	Zn(1)−N(8)	2.087(7)
Cu(1)−N(9)	1.988(8)	Zn(1)−N(10)	2.026(9)
Bond Angles (deg)			
N(1)−Cu(1)−N(3)	82.5(3)	N(2)−Zn(1)−N(4)	82.9(3)
N(1)−Cu(1)−N(5)	122.6(3)	N(2)−Zn(1)−N(6)	120.5(3)
N(1)−Cu(1)−N(7)	118.2(3)	N(2)−Zn(1)−N(8)	119.9(3)
N(1)−Cu(1)−N(9)	104.7(3)	N(2)−Zn(1)−N(10)	101.3(3)
N(3)−Cu(1)−N(5)	80.7(3)	N(4)−Zn(1)−N(6)	80.3(3)
N(3)−Cu(1)−N(7)	80.2(3)	N(4)−Zn(1)−N(8)	81.1(3)
N(3)−Cu(1)−N(9)	172.9(3)	N(4)−Zn(1)−N(10)	175.1(3)
N(5)−Cu(1)−N(7)	112.2(3)	N(6)−Zn(1)−N(8)	113.2(3)
N(5)−Cu(1)−N(9)	95.7(3)	N(6)−Zn(1)−N(10)	99.3(4)
N(7)−Cu(1)−N(9)	95.6(3)	N(8)−Zn(1)−N(10)	94.6(3)

Table 5. Selected Bond Distances and Angles of Complex **4**[a]

Bond Distances (Å)			
molecule 1		molecule 2	
Cu(1)−N(2)	2.01(1)	Cu(2)−N(8)	2.00(1)
Cu(1)−N(3)	2.03(1)	Cu(2)−N(9)	2.03(1)
Cu(1)−N(4)	2.05(1)	Cu(2)−N(10)	2.02(1)
Cu(1)−N(5)	2.07(1)	Cu(2)−N(1)	2.06(1)
Cu(1)−N(6)	2.00(1)	Cu(2)−N(12)	1.95(1)
Bond Angles (deg)			
N(2)−Cu(1)−N(3)	81.4(7)	N(8)−Cu(2)−N(9)	83.3(7)
N(2)−Cu(1)−N(4)	119.8(6)	N(8)−Cu(2)−N(10)	120.4(6)
N(2)−Cu(1)−N(5)	117.2(6)	N(8)−Cu(2)−N(11)	117.1(7)
N(2)−Cu(1)−N(6)	96.3(8)	N(8)−Cu(2)−N(12)	97.4(8)
N(3)−Cu(1)−N(4)	82.3(6)	N(9)−Cu(2)−N(10)	82.7(7)
N(3)−Cu(1)−N(5)	83.3(6)	N(9)−Cu(2)−N(11)	81.5(7)
N(3)−Cu(1)−N(6)	177.6(7)	N(9)−Cu(2)−N(12)	179.2(8)
N(4)−Cu(1)−N(5)	117.7(6)	N(10)−Cu(2)−N(11)	117.5(6)
N(4)−Cu(1)−N(6)	98.6(7)	N(10)−Cu(2)−N(12)	96.6(8)
N(5)−Cu(1)−N(6)	98.3(7)	N(11)−Cu(2)−N(12)	98.5(8)

[a] The numbering scheme for molecule 2 follows that assigned for molecule 1.

(33) Addison, A. W.; Rao, T. N.; Reedijk, J.; Rijin, J.; Verschoor, G. C. *J. Chem. Soc., Dalton Trans.* **1984**, 1349.

$O_w(2)$ atoms). The basal plane at the Cu center comprises a pyridine nitrogen, a bridged imidazolate nitrogen, a tertiary amine nitrogen, and a water oxygen. The bond lengths of complex **2** from the copper to each of donor nitrogens and oxygen are Cu(1)−N(1) 1.968(7) Å, Cu(1)−N(3) 2.027(7) Å, Cu(1)−N(5) 2.198(10) Å, Cu(1)−N(7) 2.089(8) Å, Cu(1)−O_w(1) 1.995(6) Å, Cu(2)−N(2) 1.973(8) Å, Cu(2)−N(4) 2.039(8) Å, Cu(2)−N(6) 2.186(10) Å, Cu(2)−N(8) 2.080(7) Å, and Cu(2)−O_w(2) 1.973(7) Å. It should be noted that the Cu(1)−N(5) and Cu(2)−N(6) distances in complex **2** are significantly longer than the other Cu−N(pyridine) distances in this complex, a fact which is consistent with N(5) and N(6) being the apexes of the pseudo square pyramids for Jahn−Teller distortions. It should also be noted that the Cu−Cu distance in complex **2** (6.097(2) Å) is shorter than **1** (6.197(2) Å). Such a difference in the Cu−Cu distance may be reflected in the magnetic properties as discussed later.

The Cu(II)−Zn(II) heterodinuclear complex **3** has a structure which is essentially the same as that of the corresponding Cu(II)−Cu(II) homonuclear complex **1**, as shown in Figure 1c.[34] The τ value of the Cu center of complex **3** is obtained as $\tau_1 = 0.84$ in the Cu(II) site and as $\tau_2 = 0.91$ in the Zn(II) site, where α_1 = N(1)−Cu(1)−N(5) (122.6°), β_1 = N(3)−Cu(1)−N(9) (172.9°), α_2 = N(2)−Zn(1)−N(6) (120.5°), β_2 = N(4)−Zn(1)−N(10) (175.1°), respectively. Thus, the coordination geometry of Cu(II) and Zn(II) in complex **3** can be described as slightly distorted trigonal-bipyramidal as is the case of **1**. The bond lengths of complex **3** from the copper ion to each of donor nitrogens are essentially the same as those of **1** (see Tables 2 and 4). When the Hbdpi ligand was replaced by the HMe_4-bdpi ligand, the Cu(II)−Zn(II) heterodinuclear complex could not be isolated (vide supra). The Cu(II) ion favors the square-bipyramidal coordination geometry with the HMe_4bdpi ligand as shown by the X-ray structure of complex **2** in Figure 1b, while the Zn(II) ion usually favors the trigonal-bipyramidal coordination geometry.[35] In such a case, it would be difficult to obtain the Cu(II)−Zn(II) heterodinuclear complex with the HMe_4bdpi ligand, since formation of the homodinuclear complex, which can have the same coordination geometry around each metal ion, may be favored as compared to formation of the heterodinuclear complex. On the other hand, the Cu(II)−Zn(II) heterodinuclear complex with the Hbdpi ligand was obtained selectively, since both the Cu(II) and Zn(II) ions with the Hbdpi ligand can have the same coordination geometry, i.e., trigonal bipyramid, as shown in Figure 1c.

The structure of complex **4** is quite similar to those of **1** and **3** with respect to the coordination geometry. The τ value for the Cu(II) ion of complex **4** of molecule 1[32] is obtained as $\tau = 0.96$, where α = N(2)−Cu(1)−N(4) (119.8°), β = N(3)−Cu(1)−N(6) (177.6°). Thus, the geometry of the copper ion in complex **4** can be described as a trigonal-bipyramidal structure.

Magnetic Properties of Cu(II)−Cu(II) Homodinuclear Complexes. Magnetic data for complexes **1** and **2** are shown as plots of the magnetic molar susceptibility (χ_M) and the effective magnetic moment (μ_{eff}) vs temperature (T) in Figure 3 (parts a and b, respectively). The χ_M values of complexes **1** and **2** pass through a maximum at about 65 and 130 K and then fall to a minimum at about 15 and 25 K, respectively. The μ_{eff} values of complexes **1** and **2** decrease from 1.67 and 1.54 μ_B at 300 K, which are smaller than the spin-only value (2.83 μ_B for uncoupled $S = {}^1/_2$ dimer), to 0.22 μ_B at 4.92 K and 0.11 μ_B at 20.04 K, respectively. Such behavior of χ_M and μ_{eff} of complexes **1** and **2** vs T is indicative of antiferromagnetically coupled compounds. The susceptibility data were fitted to the Bleaney−Bowers equation for exchange-coupled pairs of copper ions (eq 1),[36] where p is the paramagnetic impurity, $-2J$ is the magnetic exchange parameter in the spin Hamiltonian ($H = -2JS_1 \cdot S_2$), and g is the Landé factor. The impurity is assumed to be Cu(II) ($S = {}^1/_2$). The experimental data closely fit the equation to give the $-2J$, g, and p values for complexes **1** and **2** as given in Figure 3.

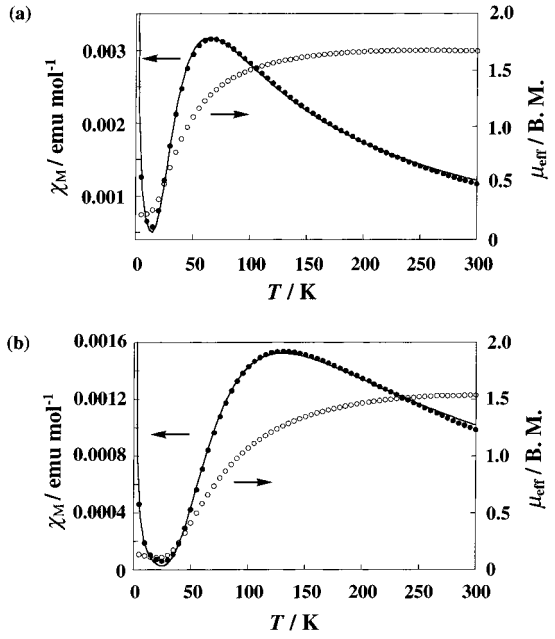

Figure 3. Temperature dependence of the molar magnetic susceptibility (χ_M) and effective magnetic moment (μ_{eff}) for (a) $[Cu_2(bdpi)(CH_3CN)_2](ClO_4)_3 \cdot CH_3CN \cdot 3H_2O$ (**1**) and (b) $[Cu_2(Me_4bdpi)(H_2O)_2](ClO_4)_3 \cdot 4H_2O$ (**2**). The solid lines result from a least-squares fit according to eq 1. The least-squares fit values for **1** and **2** are $-2J = 73.4$ and 145.9 cm^{-1}, $g = 2.10$ and 2.12, and $p = 0.016$ and 0.0069.

$$\chi_M = \frac{2Ng^2\beta^2}{kT}[3 + \exp(-2J/kT)]^{-1}(1-p) + p\frac{2Ng^2\beta^2 S(S+1)}{3kT} + \chi_{TIP} \quad (1)$$

The $-2J$ value reflects the degree of interaction between the two unpaired electrons in Cu(II) ions through the bridging imidazolate ligand and is therefore related to the structure of the complex.[37] The $-2J$ value (145.9 cm^{-1}) of complex **2** is larger than that of **1** (73.4 cm^{-1}). This can be explained by taking into account the difference in the coordination geometry between **1** and **2**. Complex **1** has an unpaired electron mainly in the d_{z^2} orbital of each Cu(II) ion with a trigonal-bipyramidal structure, while **2** has an unpaired electron mainly in the $d_{x^2-y^2}$ orbital of each Cu(II) ion with a distorted square-pyramidal structure. The overlap integral between imidazolate orbital and Cu(II) d_{z^2} orbital of complex **1** is expected to have a smaller value than

(34) Although the Cu(II) and Zn(II) ions are nearly equivalent, each position was tentatively determined as shown in Figure 1c, which gave smaller R and R_w values as compared to those of the structure when the ions were switched. A reviewer pointed out that the Cu(1)−N(3) and Zn(1)−N(4) bonds, which were identical in complex **3**, were appreciably longer than their counterparts in **1**. These facts suggest that the Cu and Zn in complex **3** are disordered over the two sites, and that the Zn−N3(4) distances are longer than the corresponding copper distances.

(35) Canary, J. W.; Allen, C. S.; Castagnetto, J. M.; Chiu, Y. H.; Toscano, P. J.; Wang, Y. *Inorg. Chem.* **1998**, *37*, 6255.

(36) Bleaney, B.; Bowers, K. D. *Proc. R. Soc. London, A* **1952**, *214*, 451.

(37) Kahn, O. *Angew. Chem., Int. Ed. Engl.* **1985**, *24*, 834.

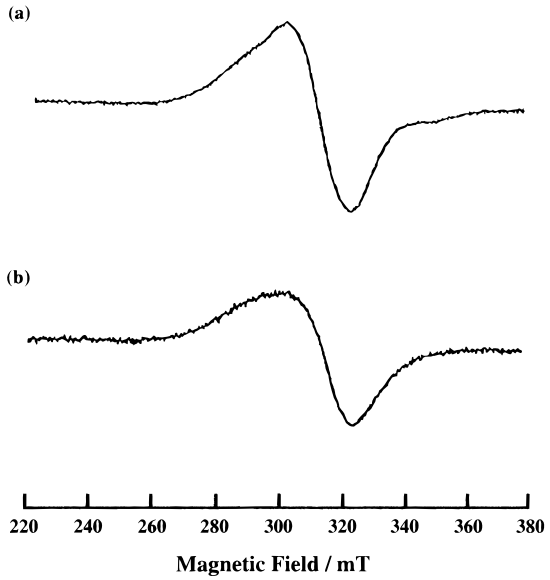

Figure 4. ESR spectra of (a) $[Cu_2(bdpi)(CH_3CN)_2](ClO_4)_3 \cdot CH_3CN \cdot 3H_2O$ (**1**, 0.5 mM; gain, 500) and (b) $[Cu_2(Me_4bdpi)(H_2O)_2](ClO_4)_3 \cdot 4H_2O$ (**2**, 0.5 mM; gain, 630) in CH_3CN/CH_3OH (1:1) at 77 K.

the overlap integral between imidazolate orbital and Cu(II) $d_{x^2-y^2}$ orbital of **2**. This may be the reason why an interaction of spin−spin coupling through the bridging imidazolate in complex **1** is smaller: to give a smaller $-2J$ value than that of **2**.

The magnitude of $-2J$ for imidazolate-bridged dicopper complexes in a square-pyramidal environment has been shown to depend on the dihedral angle (θ) between the imidazolate ring and the Cu(II) $d_{x^2-y^2}$ orbital in the square plane.[38] The smaller the θ value, the stronger the antiferromagnetic spin−spin interaction, i.e., the larger the $-2J$ value.[22] For example, small $-2J$ values have been reported for imidazolate-bridged dicopper complexes such as $[Cu_2(pip)_2(im)](ClO_4)_3$ ($-2J = 51.6$ cm^{-1}; im, imidazolate anion; pip, 2-(((2-(2-pyridyl)ethyl)imino)-methyl)imidazole)[39] and $[Cu_2(TMDT)_2(im)(ClO_4)_2]ClO_4$ ($-2J = 53.8$ cm^{-1}; TMDT, 1,1,7,7-tetramethyldiethylenetriamine),[13b] and these complexes have relatively large θ values ($\theta = 88°$ and 91°, respectively).[40] In contrast to this, a large $-2J$ value ($-2J = 163.6$ cm^{-1}) has been reported for Lippard's complex, $[Cu_2(bpim)](ClO_4)_3$ (bpim, 4,5-bis(((2-(2-pyridyl)ethyl)imino)-methyl)imidazole), which has a small θ value ($\theta = 8°$) in a square-planar environment.[41] As expected from the larger θ value ($\theta = 28°$) in complex **2** than this value, the $-2J$ value for **2** (145.9 cm^{-1}) is smaller than the value for $[Cu_2(bpim)](ClO_4)_3$ (163.6 cm^{-1}).[41] The $-2J$ values of both complexes **1** and **2** are larger than the reported value (52.0 cm^{-1}) for Cu,Cu-SOD,[42] indicating a stronger antiferromagnetic spin−spin interaction in our model complexes as compared to that in the native SOD enzyme.

ESR Spectra. The ESR spectra of complexes **1** and **2** (0.5 mM) in CH_3CN/CH_3OH (1:1) at 77 K are shown in Figure 4. Fairly broad signals centered at $g \cong 2.13$ without hyperfine structure are observed for both complexes, and such broad signals are consistent with the magnetic properties described above that indicated an antiferromagnetic spin−spin interaction.[43,44]

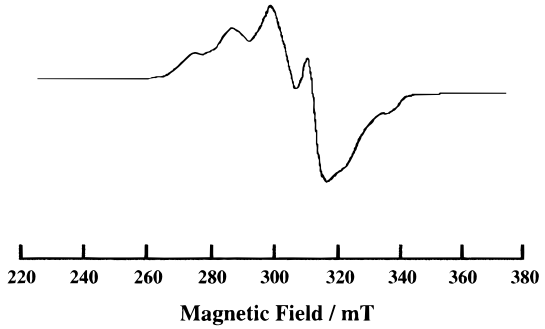

Figure 5. ESR spectrum of $[CuZn(bdpi)(CH_3CN)_2](ClO_4)_3 \cdot 2CH_3CN$ (**3**, 0.5 mM; gain, 500) in CH_3CN/CH_3OH (1:1) at 77 K.

Figure 5 shows the ESR spectrum of complex **3** (0.5 mM) in CH_3CN/CH_3OH (1:1) at 77 K, from which the well-defined ESR parameters ($g_{\|} = 2.10$, $g_{\perp} = 2.24$, $|A_{\|}| = 11.7$ mT, and $|A_{\perp}| = 12.4$ mT) are obtained. Such ESR parameters strongly indicate that the Cu(II) ion in complex **3** has a trigonal-bipyramidal environment and a d_{z^2} ground state following the criteria given by Bencini et al.,[45] in agreement with the X-ray structure in Figure 1c. The observation of a well-defined ESR spectrum of complex **3** also confirms that **3** retains its imidazolate-bridged Cu(II)−Zn(II) heterodinuclear structure and that **3** is not a 1:1 mixture of Cu(II)−Cu(II) and Zn(II)−Zn(II) homodinuclear complexes.

UV−Visible Spectra. The UV−visible spectrum of complex **1** (1.0 mM) in CH_3CN shown in Figure 6a indicates a broad d−d band consisting of two peaks centered at 645 (shoulder) and 880 nm ($\epsilon = 110$ and 420 M^{-1} cm^{-1}, respectively). The spectrum of complex **2** in Figure 6b also showed a broad d−d band consisting of two peaks centered at 640 (shoulder) and 770 nm ($\epsilon = 260$ and 360 M^{-1} cm^{-1}, respectively). In addition, the charge-transfer band from imidazolate to Cu(II) ion (LMCT) is observed at 320 and 330 nm ($\epsilon = 3000$ M^{-1} cm^{-1} in both complexes). The reflectance spectra of complexes **1** and **2** in the solid state show the same broad band, indicating that the structures of **1** and **2** in CH_3CN solution are the same as those in the solid states.

The UV−visible spectrum of complex **3** (1.0 mM) in CH_3CN shown in Figure 6c is essentially the same as the spectrum of **1** except for the ϵ values ($\epsilon = 1500$, 60, and 220 M^{-1} cm^{-1} at $\lambda_{max} = 320$, 645 (shoulder), and 880 nm, respectively), which are about one-half of those of **1**. Such a comparison of the absorption spectra between the Cu(II)−Cu(II) homodinuclear and the Cu(II)−Zn(II) heterodinuclear complexes using the same ligand has been made for the first time in this study, and the relation between **1** and **3** with respect to the λ_{max} and ϵ values is just the same as that between Cu,Cu-SOD and Cu,Zn-SOD with respect to the charge-transfer band from imidazolate to Cu(II) ($\lambda_{max} = 420$, 420 nm, $\epsilon = 272$, 134 M^{-1} cm^{-1}, respectively).[46]

Electrochemistry. Figure 7 shows cyclic voltammograms of complexes **1** and **2** (1.0 mM) in CH_3CN, which give two reversible redox waves (complex **1**, $E_{1/2a} = -0.03$ V and $E_{1/2b} = -0.31$ V; complex **2**, $E_{1/2a} = +0.12$ V and $E_{1/2b} = -0.29$ V vs Ag/AgCl). The first and second reversible waves at $E_{1/2a}$ and $E_{1/2b}$ correspond to the Cu(I,II)/Cu(II,II) and Cu(I,I)/Cu(I,II)

(38) Benelli, C.; Bunting, R. K.; Gatteschi, D.; Zanchini, C. *Inorg. Chem.* **1984**, *23*, 3074.
(39) Kolks, G.; Lippard, S. J. *J. Am. Chem. Soc.* **1977**, *99*, 5804.
(40) The averaged value is given for the θ values for two metal centers.
(41) Kolks, G.; Lippard S. J.; Waszczak, J. V.; Lilienthal, H. R. *J. Am. Chem. Soc.* **1982**, *104*, 717.
(42) Fee, J. A.; Briggs, R. G. *Biochim. Biophys. Acta* **1975**, *400*, 439.
(43) Yokoi, H.; Chikira, M. *J. Chem. Soc., Chem. Commun.* **1982**, 1125.
(44) A "$\Delta M_s = 2$" transition in the region of $g \cong 4$ was not observed because of the low intensity with the large linewidth.
(45) Bencini, A.; Bertini, I.; Gatteschi, D.; Scozzafava, A. *Inorg. Chem.* **1978**, *17*, 3194.
(46) Lu, Y.; Roe, J. A.; Bender, C. J.; Peisach, J.; Banci, L.; Bertini, I.; Gralla, E. B.; Valentine, J. S. *Inorg. Chem.* **1996**, *35*, 1692.

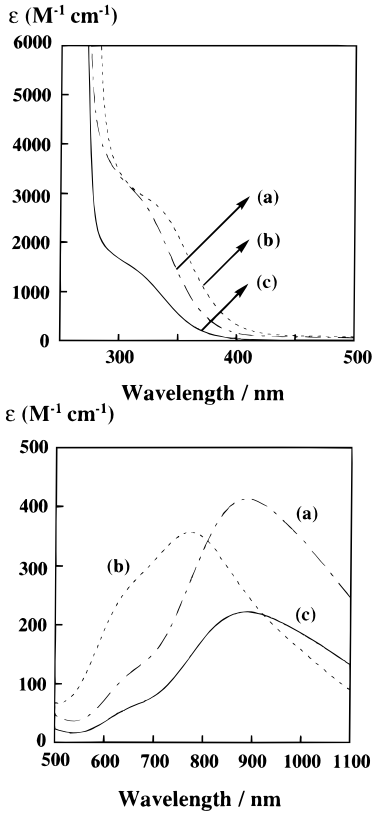

Figure 6. UV−vis spectra of (a) $[Cu_2(bdpi)(CH_3CN)_2](ClO_4)_3 \cdot CH_3CN \cdot 3H_2O$ (**1**, 0.5 mM), (b) $[Cu_2(Me_4bdpi)(H_2O)_2](ClO_4)_3 \cdot 4H_2O$ (**2**, 0.5 mM), and (c) $[CuZn(bdpi)(CH_3CN)_2](ClO_4)_3 \cdot 2CH_3CN$ (**3**, 0.5 mM) in CH_3CN at 298 K.

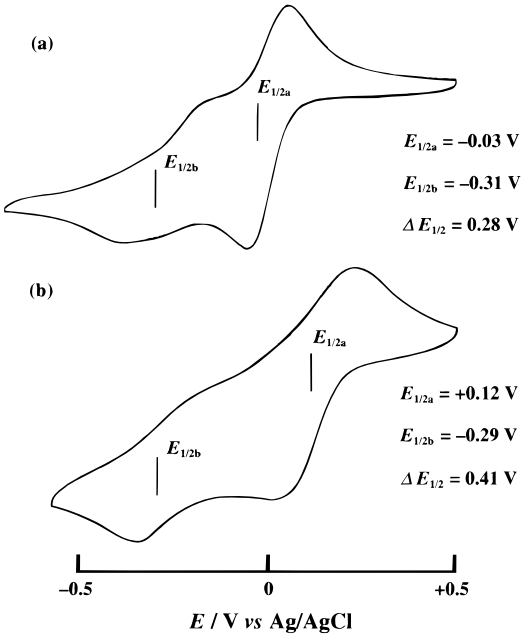

Figure 7. Cyclic voltammograms of (a) $[Cu_2(bdpi)(CH_3CN)_2](ClO_4)_3 \cdot CH_3CN \cdot 3H_2O$ (**1**, 1.0 mM) and (b) $[Cu_2(Me_4bdpi)(H_2O)_2](ClO_4)_3 \cdot 4H_2O$ (**2**, 1.0 mM) in CH_3CN containing 0.1 M TBAP. Working electrode, glassy carbon; counter electrode, Pt wire; reference electrode, Ag/AgCl; scan rate, 50 mV s^{-1}.

redox couples, respectively. The $E_{1/2a}$ value of complex **2** (0.12 V) is more positive than that of **1** (−0.03 V), but the $E_{1/2b}$ values of both complexes are nearly equal. Such a positive shift in the $E_{1/2a}$ value of complex **2** may be ascribed to the steric effect of the *o*-methyl group in the Me_4bdpi ligand in **2**, which leads to

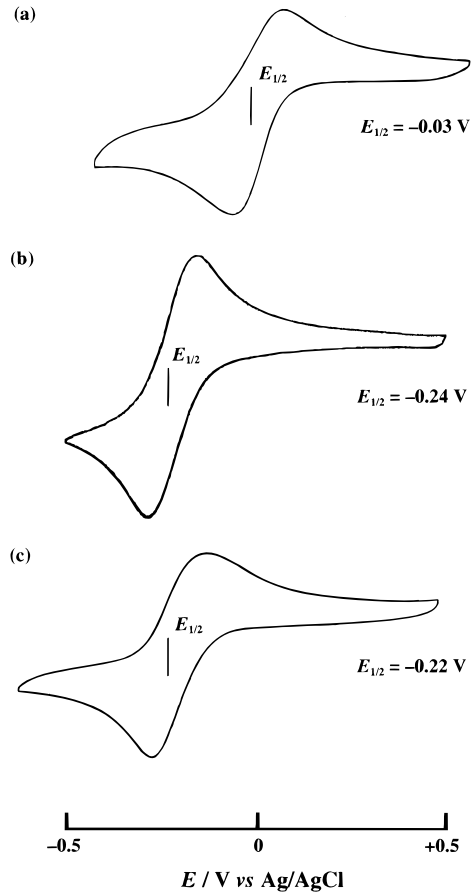

Figure 8. Cyclic voltammograms of (a) $[CuZn(bdpi)(CH_3CN)_2](ClO_4)_3 \cdot 2CH_3CN$ (**3**, 1.0 mM), (b) $[Cu(MeIm(Py)_2(CH_3CN)](ClO_4)_2 \cdot CH_3CN$ (**4**, 1.0 mM), and (c) $[Cu(Hbdpi)(CH_3CN)](ClO_4)_2$ (**5**, 1.0 mM) in CH_3CN containing 0.1 M TBAP. Working electrode, glassy carbon; counter electrode, Pt wire; reference electrode, Ag/AgCl; scan rate, 50 mV s^{-1}.

the weaker coordination to the Cu(II) ion as compared to the nonsubstituted bdpi ligand in **1**.[47] Such a steric effect of the *o*-methyl group may also result in a stronger metal−metal interaction. Since the stronger the metal−metal interaction, the larger the difference in the $E_{1/2}$ values between the first and second redox processes ($\Delta E_{1/2} = E_{1/2a} - E_{1/2b}$),[48] a larger $\Delta E_{1/2}$ value is obtained for complex **2** ($\Delta E_{1/2} = 0.41$ V) than for **1** ($\Delta E_{1/2} = 0.28$ V), as shown in Figure 7. This is consistent with the stronger spin−spin interaction in complex **2** than in **1**, as demonstrated by the larger $-2J$ value (145.9 cm^{-1}) for **2** than the value (73.4 cm^{-1}) for **1**, which were derived from the magnetic properties (vide supra).

The cyclic voltammogram (CV) of the Cu(II)−Zn(II) heterodinuclear complex **3** (1.0 mM) in CH_3CN is shown in Figure 8 (part a), where the CVs of Cu(II) mononuclear complexes, **4** and $[Cu(Hbdpi)(CH_3CN)](ClO_4)_2$ (**5**),[49] are also shown for comparison in Figure 8 (part b and c, respectively). The CV of complex **3** exhibits only one reversible Cu(I)/(II) redox couple at $E_{1/2} = -0.03$ V (vs Ag/AgCl). This also confirms that complex **3** contains one copper ion site in the complex.

The $E_{1/2}$ values of complexes **4** and **5** are nearly the same (complex **4**, $E_{1/2} = -0.24$ V; complex **5**, $E_{1/2} = -0.22$ V (vs

(47) Nagao, H.; Komeda, N.; Mukaida, M.; Suzuki, M.; Tanaka, K. *Inorg. Chem.* **1996**, *35*, 6809.

(48) Richardson, D. E.; Taube, H. *Inorg. Chem.* **1981**, *20*, 1278.

(49) To a CH_3CN solution (10 mL) of $Cu(ClO_4)_2 \cdot 6H_2O$ (3.7 mg, 1.0 mmol) was added Hbdpi (4.9 mg, 1.0 mmol) at room temperature, and the resulting solution was employed for the CV measurements.

Table 6. SOD Activities (IC_{50} Values) of Cu(II) Complexes

complex	IC_{50} (μM)[a]	ref
1	0.32	this work
2	1.1	this work
3	0.24	this work
4	0.56	this work
$[Cu(im)Cu(pip)_2]^{3+}$	0.50	17
$[Cu(im)Zn(pip)_2]^{3+}$	0.50	17
$[((Cu(im)Zn)L]^{3+}$	0.50	27d
$[Cu_2(bpzbiap)C1_3]$	0.52	26
native Cu,Zn-SOD	0.04	17

[a] The IC_{50} values for one Cu(II) ion.

Ag/AgCl)). A comparison of the $E_{1/2}$ values between the Cu(II)−Zn(II) heterodinuclear complex **3** and the corresponding Cu(II) mononuclear complexes **4** and **5** in Figure 8 (parts a, b, and c, respectively) reveals that the $E_{1/2}$ value of complex **3** is 0.21 and 0.19 V more positive than the values of the Cu(II) mononuclear complexes. Such a positive shift of the $E_{1/2}$ value of complex **3** can be ascribed to the electronic effect of the imidazolate-bound Zn(II) ion, which leads to a decrease in the electron density on the copper ion. A similar effect is also expected for another copper ion in the Cu(II)−Cu(II) homodinuclear complex **1** containing the same Hbdpi ligand. In fact, the $E_{1/2a}$ value of complex **1** (−0.03 V) shown in Figure 7a is the same as that of **3** (−0.03 V) in Figure 8a, both of which are 0.21 and 0.19 V more positive than the corresponding Cu(II) mononuclear complexes in Figure 8b and c.

SOD Activity. The Cu(II)−Cu(II) homodinuclear (**1** and **2**), Cu(II)−Zn(II) heterodinuclear (**3**), and Cu(II) mononuclear (**4**) complexes exhibit catalytic activity toward the dismutation of superoxide anions. The SOD activities of complexes **1**, **2**, **3**, and **4** were investigated by the cytochrome *c* assay[50] using the xanthine oxidase reaction as the source of superoxide. The concentrations of complexes required to attain 50% inhibition of the reduction (defined as IC_{50}) were determined for complexes **1**−**4** (see Experimental Section), and the IC_{50} values are listed in Table 6, where the values of the best SOD mimics so far reported[17,26,27d] and the value of the native SOD are also given for comparison (note that the smaller the IC_{50} value, the higher the SOD activity).

The SOD activity of dinuclear complexes increases in the order **2** < **1** < **3**. The IC_{50} value of 0.24 μmol dm^{-3} determined for complex **3** is still larger than the value reported for native SOD (0.04 μM) but smaller than the best reported value. Thus, our imidazolate-bridged Cu(II)−Zn(II) heterodinuclear SOD model complex **3**, which has a coordination site available for the binding of superoxide as shown by the X-ray structure in Figure 1c, exhibits *the highest activity* among the structurally established SOD models reported so far. In addition, The IC_{50} value for Cu(II) mononuclear complex **4** is determined to be 0.56 μM. The difference in IC_{50} values between complex **3** and **4** may be ascribed to the imidazolate bridge and zinc ion.

(50) Fridovich, I.; Beauchamp, C. *Anal. Biochem.* **1971**, *44*, 276.

Conclusion

The imidazolate-bridged Cu(II)−Zn(II) heterodinuclear SOD model complex **3**, which has a coordination site available for the binding of superoxide as shown by the X-ray structure in Figure 1c, exhibits *the highest activity* among the structurally established SOD models reported so far. A large positive shift (0.21 and 0.19 V) on the $E_{1/2}$ value of the imidazolate-bridged Cu(II)−Zn(II) heterodinuclear complex **3** is clearly shown by comparison with the $E_{1/2}$ values of the corresponding Cu(II) mononuclear complexes **4** and **5**. Thus, an important role of Zn(II) ion in the imidazolate-bridged Cu(II)−Zn(II) heterodinuclear complex **3** may be to accelerate an outer-sphere electron transfer from superoxide to **3** to produce the Cu(I)−Zn(II) complex when the free energy change of electron transfer for **3** becomes thermodynamically more favorable as compared to that without Zn(II) ion. The presence of a Zn(II) ion which can act as a Lewis acid may also be able to accelerate an electron transfer from the Cu(I)−Zn(II) complex to superoxide, since superoxide is known to form a complex with metal ions acting as a Lewis acid to accelerate the electron-transfer reduction of superoxide.[51] Such an acceleration for the reduction of superoxide can also be attained by a Brønsted acid instead of a Lewis acid since Valentine et al. reported that the reduction of superoxide for the zinc-deficient SOD form is acid-catalyzed.[8,52] Thus, the essential role of Zn(II) ion in SOD seems to be to accelerate both the oxidation and the reduction of superoxide by controlling the redox potentials of Cu(II) ion and superoxide in the catalytic cycle of SOD.

Acknowledgment. We are grateful to Prof. Hiromu Sakurai, Kyoto Pharmaceutical University, for the measurements of the SOD activity and Sachiyo Nomura, Institute for Molecular Science, for measurements of ICP. This work was partially supported by Grants-in-Aid for Scientific Research Priority Area (Nos. 11228205 and 11136229 to S.F.) and Grants-in-Aid for Scientific Research (No. 09304062 to O.Y. and No. 07CE2004-(COE) to A.O.) from the Ministry of Education, Science, Culture and Sports, Japan.

JA994050J

(51) (a) Fukuzumi, S.; Patz, M.; Suenobu, T.; Kuwahara, Y.; Itoh, S. *J. Am. Chem. Soc.* **1999**, *121*, 1605. (b) Fukuzumi, S.; Okamoto, T. *J. Chem. Soc., Chem. Commun.* **1994**, 29. (c) Itoh, S.; Kawakami, H.; Fukuzumi, S. *Chem. Commun.* **1997**, 29.

(52) For acid-catalyzed reduction of oxygen, see: (a) Fukuzumi, S. In *Advances in Electron-Transfer Chemistry*; Mariano, P. S., Ed.; JAI: Greenwich, CT, 1992; Vol. 2, pp 67−175. (b) Fukuzumi, S.; Itoh, S. In *Advances in Photochemistry*; Volman, D., Hammond, G. S., Neckers, D. C., Eds.; Wiley: New York, 1999; Vol 25, pp 107−172.